

## Hsa\_circ\_0053063 inhibits breast cancer cell proliferation via hsa\_circ\_0053063/hsa-miR-330-3p/PDCD4 axis

Changle Ji<sup>1,2,\*</sup>, Jiashu Hu<sup>1,2,\*</sup>, Xuehui Wang<sup>1,3</sup>, Wenfang Zheng<sup>1,2</sup>, Xiaochong Deng<sup>1,2</sup>, Hongming Song<sup>1,4</sup>, Yunhe Yu<sup>1,2</sup>, Qifeng Luo<sup>1</sup>, Kaiyao Hua<sup>1,2</sup>, Xiqian Zhou<sup>1,2</sup>, Lin Fang<sup>1</sup>

<sup>1</sup>Department of Breast and Thyroid Surgery, Shanghai Tenth People's Hospital, Tongji University School of Medicine, Shanghai 200072, China

<sup>2</sup>Tongji University School of Medicine, Shanghai 200092, China

<sup>3</sup>Nanjing Medical University, Nanjing 211166, China

<sup>4</sup>Breast Disease Center, The Affiliated Hospital of Qingdao University, Qingdao 266000, Shandong, China

\*Equal contribution

**Correspondence to:** Lin Fang; email: [1200038@tongji.edu.cn](mailto:1200038@tongji.edu.cn)

**Keywords:** breast cancer, hsa\_circ\_0053063, hsa-miR-330-3p, PDCD4, ceRNA, HADHA

**Received:** June 24, 2020

**Accepted:** February 13, 2021

**Published:** March 19, 2021

**Copyright:** © 2021 Ji et al. This is an open access article distributed under the terms of the [Creative Commons Attribution License](https://creativecommons.org/licenses/by/3.0/) (CC BY 3.0), which permits unrestricted use, distribution, and reproduction in any medium, provided the original author and source are credited.

### ABSTRACT

Breast cancer (BC) is one of the most common malignancies and its mortality is the highest among females. Circular RNAs (circRNAs), a novel group of non-coding RNAs, play an important regulatory role in angiogenesis and cancer progression. Hsa\_circ\_0053063 is a circRNA generated from several exons of HADHA. The potential role of hsa\_circ\_0053063 in BC remains unknown and needs to be explored. Hsa\_circ\_0053063 was mainly located in the cytoplasm and activated in BC tissues and cell lines. The binding position between hsa\_circ\_0053063 and miR-330-3p was confirmed by luciferase reporter assay. Moreover, hsa\_circ\_0053063 inhibited cell viability, proliferation, and progression of BC through the negative regulation of miR-330-3p. Programmed cell death 4 (PDCD4) is a direct target of miR-330-3p. Besides, the over-expression of miR-330-3p promoted cell progression by directly targeting and regulating PDCD4. Mechanistically, hsa\_circ\_0053063 activated PDCD4 by targeting miR-330-3p to inhibit BC progression. In conclusion, hsa\_circ\_0053063 inhibits breast cancer cell proliferation via hsa\_circ\_0053063/hsa-miR-330-3p/PDCD4 axis, which may provide a new therapeutic target for BC patients.

### INTRODUCTION

Breast cancer (BC) is a major disease that threatens women's health. The incidence (24.2%) and mortality (15.0%) are higher than other cancers worldwide for females based on GLOBOCAN database (2018) [1]. In recent years, more diagnostic and therapeutic methods of BC have been developed. However, the incidence rate and death rate of BC have not decreased [2]. Metastasis, recrudescence, and drug resistance are very common in BC and have caused many relative deaths.

Therefore, exploring the molecular mechanism of BC is still a vital task.

Recent studies indicated that non-coding RNAs (ncRNAs) take part in mediating BC genesis and progression [3]. MicroRNAs (miRNAs), such as miR-200b, miR-497, and miR-21, regulate BC-related gene expression mainly through post-transcriptional ways [4–6]. Long non-coding RNAs (lncRNAs) including lncRNA LINK-A and lncRNA POU3F3 affect the genesis, metabolism, proliferation, and apoptosis of BC

[7, 8]. Circular RNAs (circRNAs) are novel ncRNAs with closed continuous loops formed by back splicing [9]. The first circRNA was discovered in 1976. At that time, circRNAs were regarded as mis-splicing or by-products of pre-mRNA processing for a long while [10, 11]. Nowadays, a great number of circRNAs have been detected and their biological functions are partly uncovered. The underlying mechanism of circRNAs' functions mainly includes miRNA or protein sponges, enhancer of protein function, protein scaffolding, protein recruitment, and templates for peptides translation [12]. As for tumors, some studies revealed that circRNAs could participate in tumorigenesis and they may be the potential biomarkers and therapeutic targets of cancers [10, 12]. Therefore, the regulatory function of circRNAs in BC is worthy to study.

PDCD4 (Programmed Cell Death 4), was cloned from the human library by Matsushashi's group in 1997 [13]. Then in 1999, PDCD4 was firstly described as a tumor suppressor by Cmarik's group, which found that PDCD4 could inhibit neoplastic transformation in mouse JB6 cells [14]. The human PDCD4 gene is located on chromosome 10q24 and encoded by 185 amino acids. In

recent years, PDCD4 has been found to participate in the oncogenesis and progression of BC cells [15, 16]. Study on enhancing the activity of PDCD4 may bring an advance in the treatment of BC [17].

In this study, we found a highly expressed circRNA in BC, hsa\_circ\_0053063 and then we exposed it as a tumor suppressor via negative regulating miR-330-3p expression to activate PDCD4. This provided new insight into BC treatment.

## RESULTS

### Characterization of hsa\_circ\_0053063 in BC cells

Data from high throughput sequencing chip GSE101123 in GEO (<https://www.ncbi.nlm.nih.gov/geo/>) indicated that hsa\_circ\_0053063 is highly expressed in BC tissues than in adjacent normal ones. According to the UCSC (<http://genome.ucsc.edu/>), hsa\_circ\_0053063 has a spliced length of 362 bp and is generated from the 5th-7th exon of the gene HADHA, which is located at chr2:26453059-26457223 (Figure 1A). When oligo (dT)18 primers were used, the expression of

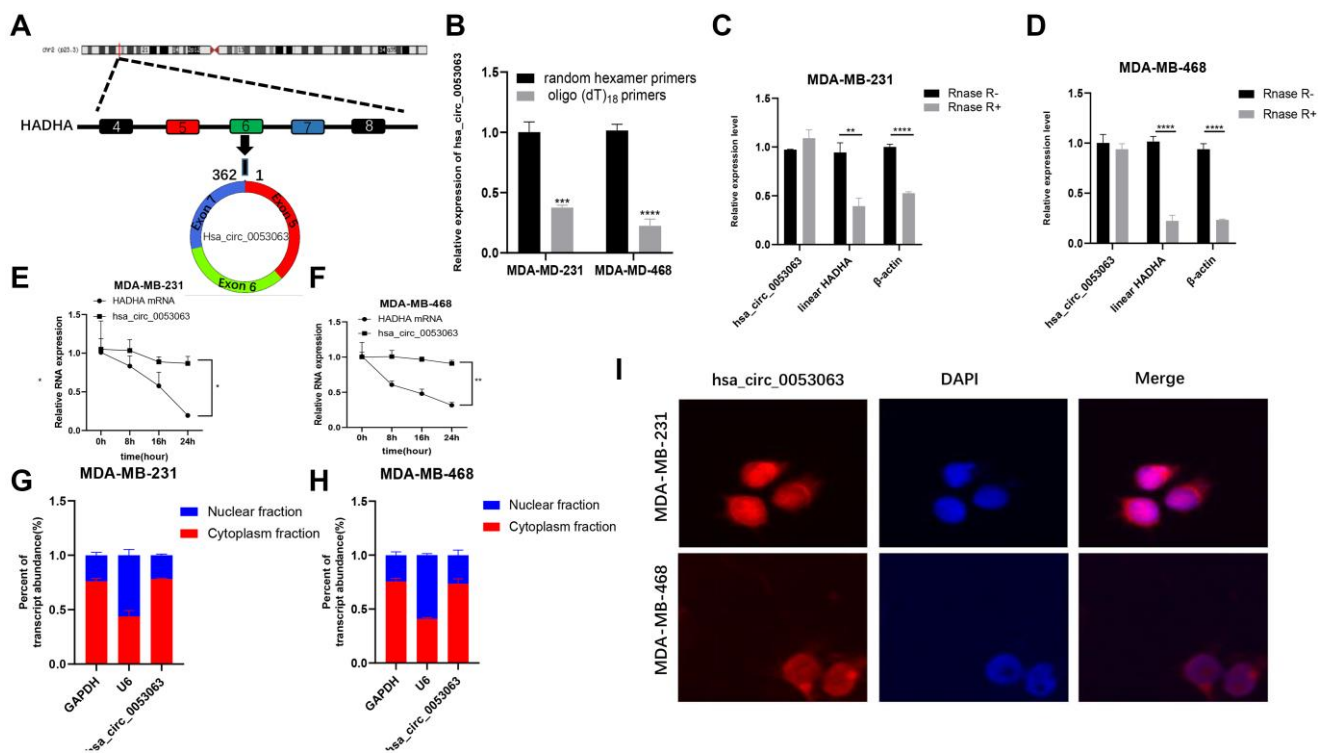


**Figure 1. Characterization of hsa\_circ\_0053063 in BC cells.** (A) Hsa\_circ\_0053063 is composed of exon 5-7 of gene HADHA. (B) qRT-PCR was used to test the expression of hsa\_circ\_0053063 in MDA-MB-231 and MDA-MB-468 cells with random hexamer or oligo (dT)18 primers. (C–D) qRT-PCR analysis revealed the expression of hsa\_circ\_0053063, linear HADHA, and  $\beta$ -actin in MDA-MB-231 and MDA-MB-468 cells treated with or without RNase R. (E–F) Expression of PDCD4 mRNA level and hsa\_circ\_0053063 in MDA-MB-231 and MDA-MB-468 cells treated with actinomycin D. (G–H) Expression levels of GAPDH, U6, and hsa\_circ\_0053063 in the cell cytoplasmic and nuclear were determined by qRT-PCR in MDA-MB-231 and MDA-MB-468 cells. (I) RNA FISH for hsa\_circ\_0053063, and nuclei was stained with DAPI. (\* $p < 0.05$ , \*\* $p < 0.01$ , \*\*\* $p < 0.001$ , \*\*\*\* $p < 0.0001$ ).

**Table 1. The relationship between the expression of hsa\_circ\_0053063 and various clinicopathological variables.**

Patients Characteristics	Total	hsa_circ_0053063 expression		
		High (N = 25)	Low (N = 5)	P value*
Age				0.0455*
<60	18	17	1	
≥60	12	8	4	
TNM stage				0.33669
I and II	26	21	5	
III and IV	4	4	0	
Lymph node metastasis				0.23556
negative	19	17	2	
positive	11	8	3	
Tumor size(cm)				0.51248
≤2	14	11	3	
>2	16	14	2	
Recrudescence				0.71229
No	22	18	4	
Yes	8	7	1	

hsa\_circ\_0053063 decreased in MDA-MB-231 and MDA-MB-468 cell lines compared with random hexamer primers. This result meant that hsa\_circ\_0053063 lacked the 3'poly-A tail and had a unique closed-loop structure (Figure 1B). Besides, the total RNA of MDA-MB-231 and MDA-MB-468 cells were treated with Rnase R exonuclease, through qRT-PCR, the results verified that hsa\_circ\_0053063 has a circular structure in these two cell lines (Figure 1C–1D). To confirm the stability of hsa\_circ\_0053063, the relative expression of HADHA mRNA level was reduced by about 70% while there was almost no decrease of hsa\_circ\_0053063 after treatment with actinomycin D for 24 h (Figure 1E–1F). Moreover, qRT-PCR was used to explore the relative expression levels of GAPDH (cytoplasmic control transcripts), U6 (nuclear control transcript), and hsa\_circ\_0053063 in the cytoplasm and nuclear fractions from MDA-MB-231 and MDA-MB-468 cells. The results indicated that hsa\_circ\_0053063 was enriched in the cytoplasm (Figure 1G–1H). This is also confirmed by the FISH analysis (Figure 1I).

### **Hsa\_circ\_0053063 is highly expressed in BC and acts as an antioncogene in BC cells**

qRT-PCR was used to measure the relative expression of hsa\_circ\_0053063 in 30 pairs of BC tissues and normal tissues, which results demonstrated that hsa\_circ\_0053063 was increased in BC tissues (24/30, 80%) (Figure 2A). Moreover, compared with MCF-10A, the relative

expression of hsa\_circ\_0053063 was also increased in 4 BC cell lines (Figure 2B). Given the results above, we chose MDA-MB-231 and MDA-MB-468 cell lines for subsequent experiments. To explore the function of hsa\_circ\_0053063 in BC, we used siRNA (si-circ\_0053063) to inhibit hsa\_circ\_0053063 function in the MDA-MB-231 and MDA-MB-468 cells. Also, we used qRT-PCR to confirm the transfection efficiency of this specific siRNA (Figure 2C). Both MTT and colony formation assays showed that si-circ\_0053063 increased cell proliferation in the MDA-MB-231 and MDA-MB-468 cells (Figure 2D–2G). Western blot analysis demonstrated that PCNA, a proliferation marker, could be raised by si-circ\_0053063 (Figure 2H–2I). Besides, we stably overexpressed hsa\_circ\_0053063 in these two cell lines (Figure 2J). MTT and colony formation assays were used to prove over-expression hsa\_circ\_0053063 could inhibit BC cell proliferation (Figure 2K–2N). To investigate whether there is a connection between the expression of hsa\_circ\_0053063 and multiple clinic pathological variables, these 30 patients' clinical data were used for analysis. Results showed that hsa\_circ\_0053063 high expression was only positively related to the age of these patients. Due to its small sample size, this connection needs to be further verified (Table 1).

### **Hsa\_circ\_0053063 inhibits BC tumor growth *in vivo***

The xenograft tumor assay was performed to verify the function of hsa\_circ\_0053063 *in vivo*. MDA-MB-231

cells were stably transfected with lv-circ\_0053063 or lv-NC. The expression of hsa\_circ\_0053063 was verified by qRT-PCR (Figure 3A). The mice were

injected with these two group cells (Figure 3B). The mice tumors were photographed, measured, and weighed. The mice tumors of the lv-circ\_0053063

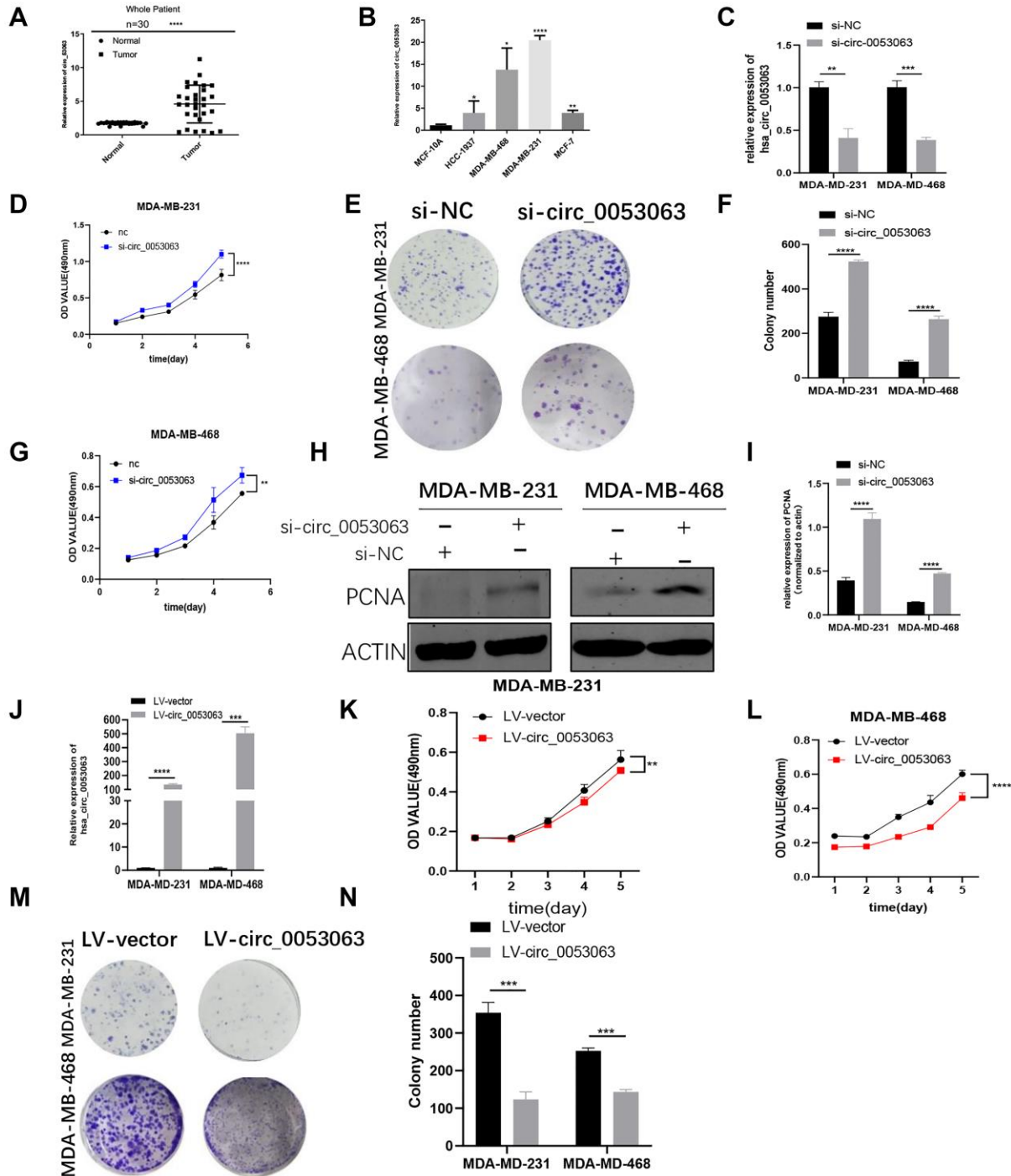


**Figure 2. Hsa\_circ\_0053063 is highly expressed in BC and acts as an antioncogene in BC cells.** (A) qRT-PCR analysis revealed the expression of hsa\_circ\_0053063 in BC tissues and adjacent normal tissues. (B) Relative expression of hsa\_circ\_0053063 in BC cell lines compared with normal breast epithelial cell line MCF-10A. (C) qRT-PCR analysis revealed the transfection efficiency of hsa\_circ\_0053063 specific siRNA. (D–G) Effect of siRNA targeting hsa\_circ\_0053063 on MTT assays and colony formation in MDA-MB-231 and MDA-MB-468 cells. (H–I) Western blot analysis demonstrated the effect of hsa\_circ\_0053063 siRNAs on PCNA in MDA-MB-231 and MDA-MB-468 cell lines. (J) qRT-PCR revealed the overexpression efficiency of LV-circ\_0053063 in MDA-MB-231 and MDA-MB-468 cell lines. (K–N) Effect of LV-circ\_0053063 on proliferation in MDA-MB-231 and MDA-MB-468 cell lines by MTT assay and colony formation assays. (\* $p < 0.05$ , \*\* $p < 0.01$ , \*\*\* $p < 0.001$ , \*\*\*\* $p < 0.0001$ ).

group are significantly smaller than the control group (Figure 3C–3D). Immunohistochemistry assay revealed PDCD4 protein expression was higher in the hsa\_circ\_0053063 overexpression group (Figure 3E–3F). Through the results above, we proved that hsa\_circ\_0053063 can inhibit BC tumor growth.

### Hsa\_circ\_0053063 inhibited the expression of miR-330-3p

During the past several years, there have been many studies on how circRNAs work as miRNA sponges to realize the function. In consideration of hsa\_circ\_0053063 is mainly located in the cytoplasm, we assumed that hsa\_circ\_0053063 inhibits breast cancer cell proliferation through realizing function by acting as a ceRNA. Four databases, Starbase (<https://web.archive.org/web/20110222111721/http://starbase.sysu.edu.cn/>), CircInteractome (<https://circinteractome.nia.nih.gov/>), Miranda and RNAhybird (<http://bibiserv.techfak.uni-bielefeld.de/rnahybrid/>) were employed to predict potential miRNA binding target of hsa\_circ\_0053063. We integrated these data into a Wynn diagram and chose mRNAs from intersections of at least three databases, in the end, 6 miRNAs (miR-874-3p, miR-431-5p, miR-18182, miR-940, miR-346, miR-330-3p) were selected (Figure 4A–4B). Then, qRT-PCR was used to verify whether miRNAs' expression can be inhibited by hsa\_circ\_0053063. Results indicated that both in MDA-MB-231 and MDA-MB-468 cell lines, only miR-330-3p presented a negative correlation with hsa\_circ\_0053063,

which suggested that hsa\_circ\_0053063 acts as a ceRNAs to bind miR-330-3p (Figure 4C–4D). Negatively correlations between the expression of hsa\_circ\_0053063 and miR-330-3p were found in 30 BC samples (Supplementary Figure 1A). As predicted by CircInteractome, hsa\_circ\_0053063 contained the putative bind sites for miR-330-3p (Figure 4E). We confirm that hsa\_circ\_0053063 could directly bind to miR-330-3p through dual-luciferase assays. Overexpression of miR-330-3p decreased the luciferase activity of wild-type hsa\_circ\_0053063, while it did not have any influence on the luciferase activity of mutation-type hsa\_circ\_0053063 (Figure 4F). Therefore, these data indicated that hsa\_circ\_0053063 directly binds to miR-330-3p.

### MiR-330-3p highly expresses and acts as an oncogene in BC cells

To further explore the function of miR-330-3p in BC, the miR-330-3p expression level was tested by using qRT-PCR in BC cell lines. A significant trend of high expression was observed in BC patient tissues and cell lines, which implied that miR-330-3p may act as an oncogene in BC cells (Figure 5A–5B). To verify the function of miR-330-3p, MTT assays and colony formation assays were performed in MDA-MB-231 and MDA-MB-468 cell lines. The results indicated that miR-330-3p mimics could promote the proliferation of BC cells while miR-330-3p inhibitor was on the opposite (Figure 5C–5H). Also, western blot results showed that PCNA expression was raised by miR-330-3p

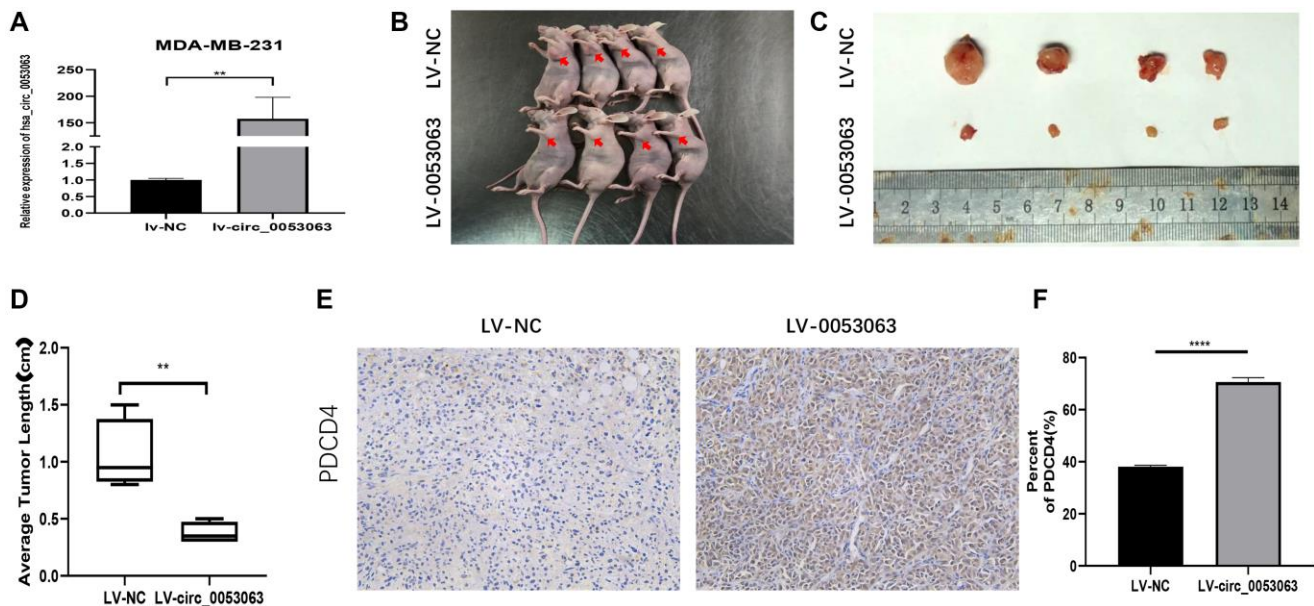


**Figure 3. Hsa\_circ\_0053063 inhibits BC tumor growth *in vivo*.** (A) Hsa\_circ\_0053063 overexpression efficiency in MDA-MB-231 cells was affirmed by qRT-PCR. (B) The nude mice injected into the fat pad of the right second breast. (C–D) The mice tumors were photographed and measured. (E–F) IHC assay revealed PDCD4 protein expression in the over-expression group and NC group. (\* $p < 0.05$ , \*\* $p < 0.01$ , \*\*\* $p < 0.001$ , \*\*\*\* $p < 0.0001$ ).

mimics (Figure 5I–5J). These results demonstrated that miR-330-3p could accelerate the proliferation function of BC cells.

### PDCD4 served as a molecular target of miR-330-3p

We found PDCD4 was a putative target of miR-330-3p by TargetScan ([http://www.targetscan.org/vert\\_71/](http://www.targetscan.org/vert_71/)). It has been proved that PDCD4 is a target gene of miR-330-3p in human esophageal cancer [18]. Results from qRT-PCR demonstrated that PDCD4 presented with low expression in BC patient tissues and BC cell lines (Supplementary Figure 1B–1C). So we conjectured that hsa\_circ\_0053063 inhibits BC cell proliferation through targeting the miR-330-3p/PDCD4 axis in BC. Through dual-luciferase assays, we confirmed that PDCD4 was the direct target of miR-330-3p (Figure 6A). The wild and mutant dual-luciferase reporter plasmids of PDCD4 were constructed, and the data indicated that miR-330-3p mimics reduced the luciferase activity of the PDCD4-WT luciferase reporter but not that of mutant ones (Figure 6B). Then, PDCD4 expression was tested in both BC tissues and cell lines through qRT-PCR, which results demonstrated that PDCD4 was low-expressed in BC

(Figure 6C–6D). Furthermore, to verify the function of PDCD4 in BC, PDCD4 siRNA was used to transfect BC cell lines. Through MTT and colony formation assays, the results indicated that PDCD4 could inhibit cell proliferation in BC (Figure 6E–6H).

### Hsa\_circ\_0053063 activated PDCD4 through targeting miR-330-3p

To further explore whether hsa\_circ\_0053063 could activate the expression of PDCD4 or not. First, the relative expression of miR-330-3p and PDCD4 were detected by qRT-PCR in MDA-MB-231 and MDA-MB-468 cells infected by si-circ\_00053063 and LV-circ\_0053063 (Figure 7A–7B). The results showed that si-circ\_0053063 could increase the expression of miR-330-3p meanwhile decrease the expression of PDCD4. In the meanwhile, lv-circ\_0053063 could do the opposite. On the other hand, qRT-PCR results revealed that miR-330-3p could reduce the expression level of PDCD4 mRNA, while the miR-330-3p inhibitor got opposite results (Figure 7C–7D). To confirm that hsa\_circ\_0053063 and miR-330-3p could influence PDCD4 on the protein level, western blot assays were employed. The results demonstrated that when

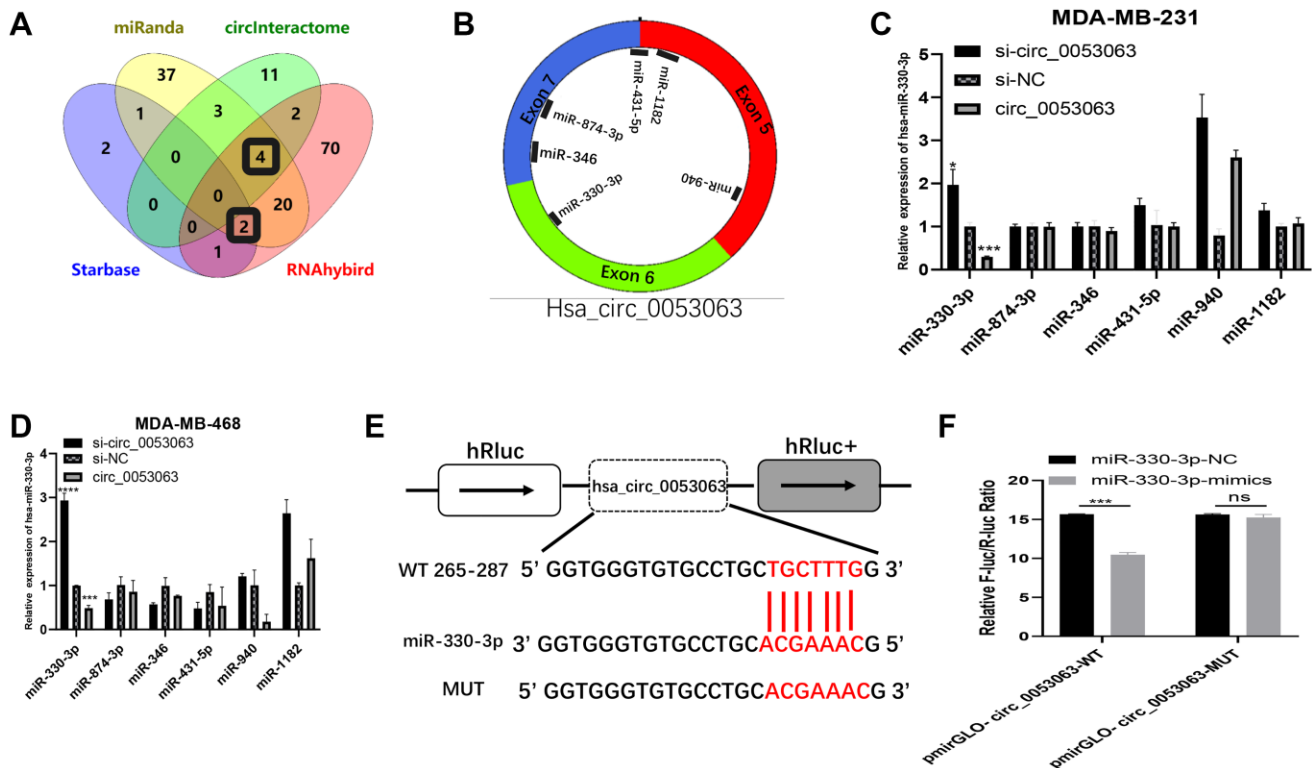


**Figure 4. Hsa\_circ\_0053063 inhibited the expression of miR-330-3p.** (A–B) Databases were employed to predict potential miRNA target of hsa\_circ\_0053063 and Venn diagram showed the target miRNAs from intersections (miR-330-3p, miR-346, miR-431-5p, miR-874-3p, miR-1182). (C–D) qRT-PCR was used to verify which miRNAs can be regulated by hsa\_circ\_053063 in MDA-MB-231 and MDA-MB-468 cell lines. (E) Predicted binding sites of hsa\_circ\_0053063 for miR-330-3p. (F) Dual-luciferase reporter assay evaluating the interaction between wild-type hsa\_circ\_0053063 + miR-330-3p reporter compared with mutant hsa\_circ\_0053063+ miR-330-3p reporter. (\* $p < 0.05$ , \*\* $p < 0.01$ , \*\*\* $p < 0.001$ , \*\*\*\* $p < 0.0001$ ).

transfected with lv-circ\_0053063, the protein levels of PDCD4 were increased, while the results were, on the contrary when transfected with miR-330-3p mimics (Figure 7E–7H). Collectively, hsa\_circ\_0053063 could activate PDCD4 through targeting miR-330-3p.

### Hsa\_circ\_0053063 generated the anti-oncogenic function in BC cells via the regulation of miR-330-3p/PDCD4 axis

To explore the biological function of the hsa\_circ\_0053063-miR-330-3p-PDCD4 axis and verify

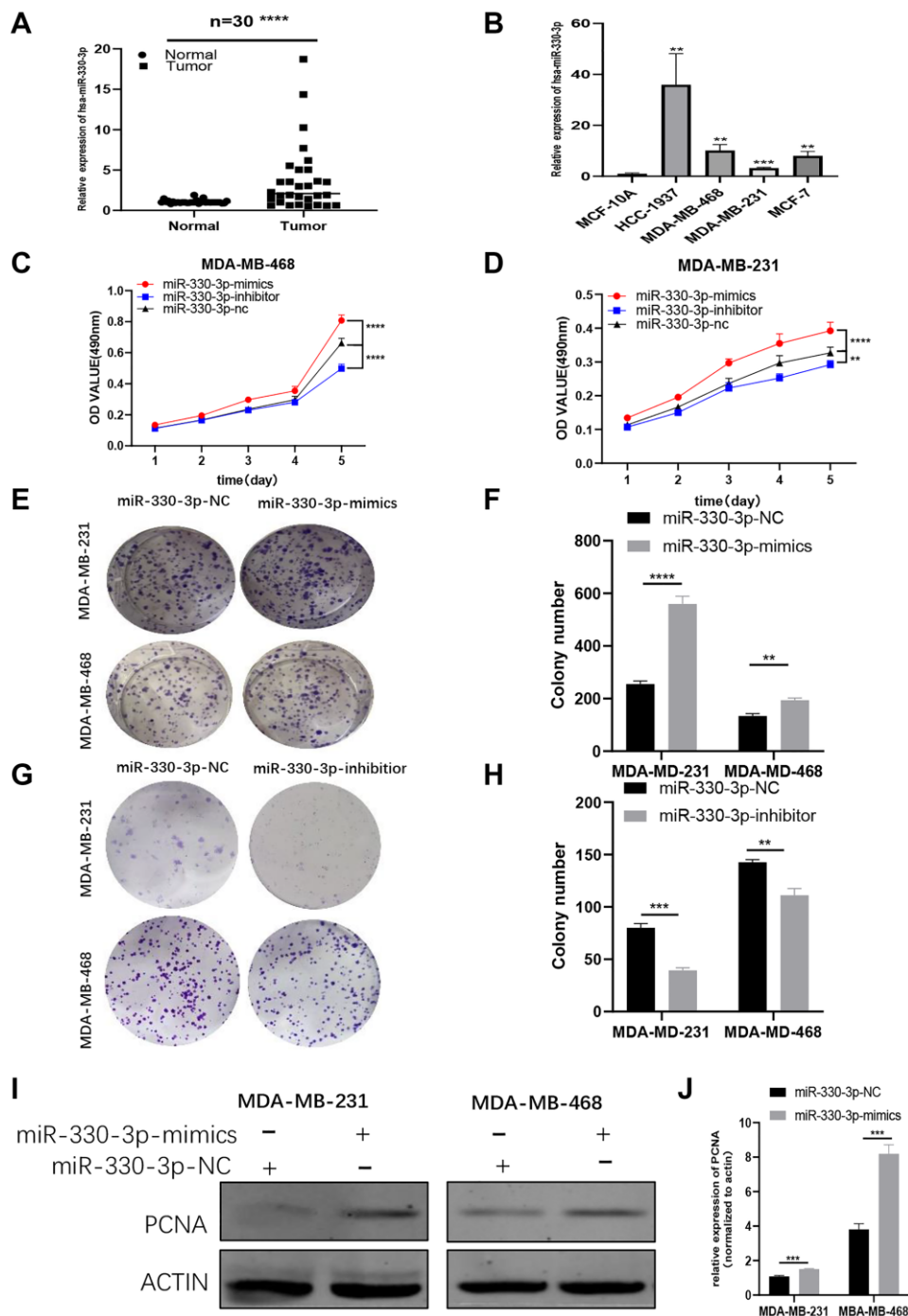


**Figure 5. MiR-330-3p highly expresses and acts as an oncogene in BC cells.** (A–B) QRT-PCR assays revealed miR-330-3p expression in BC patient tissues and BC cell lines. (C–H) MTT assays and colony formation assays were performed in MDA-MB-231 and MDA-MB-468 cell lines to determine the effect of miR-330-3p-inhibitor and miR-330-3p-mimics on proliferation. (I–J) Effect of miR-330-3p-mimics on proliferation in MDA-MB-231 and MDA-MB-468 cells by western blot. (\* $p < 0.05$ , \*\* $p < 0.01$ , \*\*\* $p < 0.001$ , \*\*\*\* $p < 0.0001$ ).

that hsa\_circ\_0053063 could increase PDCD4 protein level by absorbing miR-330-3p in BC, we performed rescue assays in MDA-MB-231 and MDA-MB-468 cell lines. According to the results of MTT assays, the hsa\_circ\_0053063-induced negative effects on proliferation were relieved after transfected with miR-330-3p mimics (Figure 8A–8B). Moreover, according to western blot assays, the increased protein level of PDCD4 induced by hsa\_circ\_0053063 was alleviated by miR-330-3p (Figure 8C–8F). The PCNA protein level also indicated that miR-330-3p mimics could reveal the decreased cell proliferation of BC cells induced by hsa\_circ\_0053063. In a word, we confirmed that hsa\_circ\_0053063 generated the anti-oncogenic function in BC cells via the miR-330-3p/PDCD4 axis regulation.

### Hsa\_circ\_0053063 inactivated P53 through miR-330-3p/PDCD4 axis

PDCD4 can suppress the translation of P53 mRNA [19]. Therefore, western blot was employed to explore whether hsa\_circ\_0053063 could inactivate P53 through

miR-330-3p/PDCD4 axis. The results showed that si-circ\_0053063 could induce P53 protein enrichment (Figure 9A–9B). PDCD4 siRNA could also accrete the P53 protein level (Figure 9C–9D). Further investigation showed that the decreased protein level of P53 induced by hsa\_circ\_0053063 can be alleviated by miR-330-3p mimics which indicated that hsa\_circ\_0053063 inactivated P53 through miR-330-3p/PDCD4 axis (Figure 9E–9G).

### The mechanism diagram shows how hsa\_circ\_0053063 inhibits BC cells proliferation by miR-330-3p as a ceRNA

Taken together, hsa\_circ\_0053063 inhibits the expression of miR-330-3p, thus it could activate one of miR-330-3p's downstream genes PDCD4 through targeting miR-330-3p. So hsa\_circ\_0053063 generated the anti-oncogenic function in BC cells via regulating miR-330-3p/PDCD4 axis. The mechanism diagram illustrates how this axis works and this study provided a new clinical diagnostic and therapeutic target of BC (Figure 10).

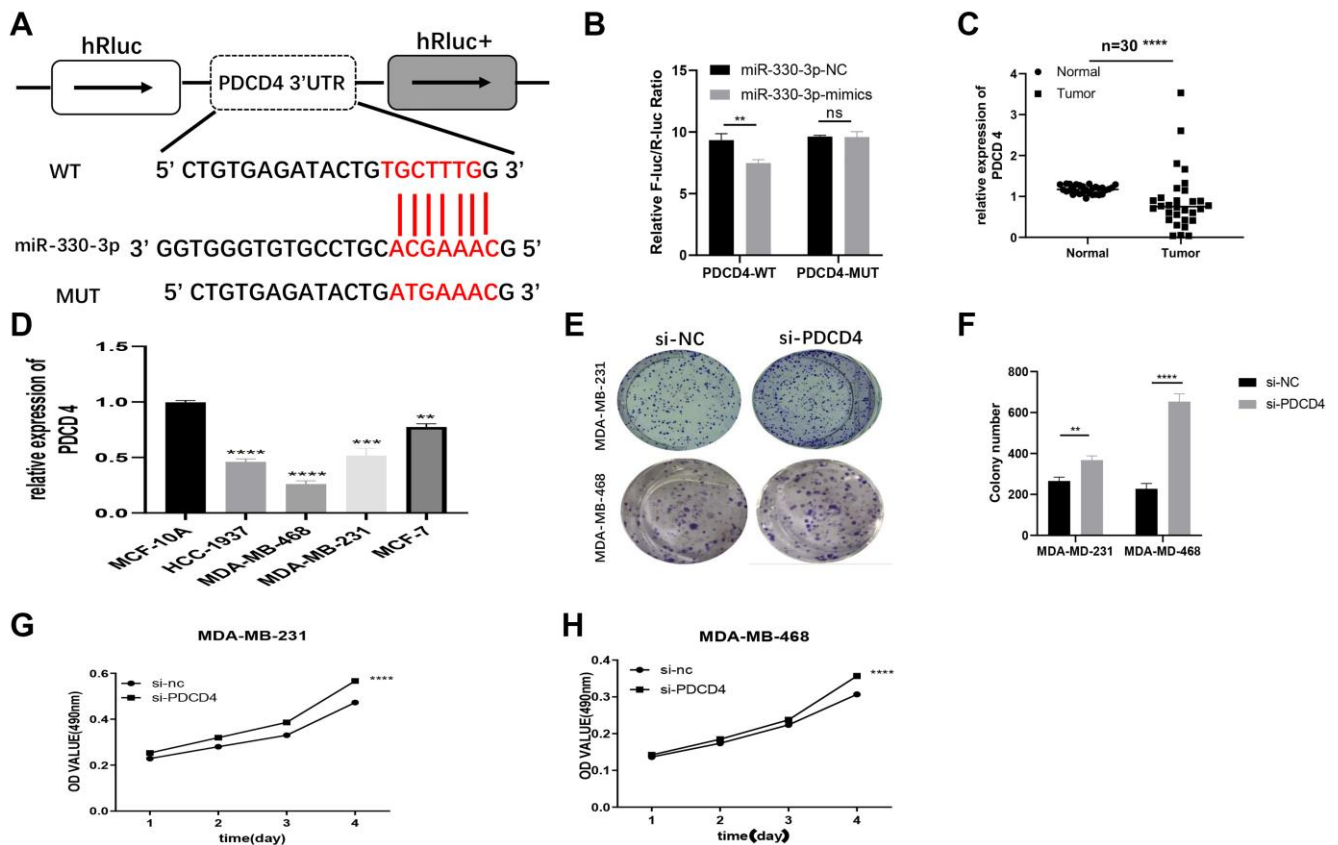


**Figure 6. PDCD4 served as a molecular target of miR-330-3p.** (A) Putative complementary sites within PDCD4 and R-330-3p predicted by TargetScan. (B) Dual-luciferase reporter assay evaluates the interaction between wild-type PDCD4 + miR-330-3p reporters compared with mutant PDCD4+ miR-330-3p reporter. (C–D) The expression levels of PDCD4 were tested in both BC tissues and cell lines through QRT-PCR. (E–H) Effect of siRNA targeting PDCD4 on colony formation and MTT assays in MDA-MB-231 and MDA-MB-468 cell lines. (\* $p < 0.05$ , \*\* $p < 0.01$ , \*\*\* $p < 0.001$ , \*\*\*\* $p < 0.0001$ ).



## DISCUSSION

First found in viruses, then proved to be presented in eukaryotic cells, circular RNAs (circRNAs) are a

species of non-coding RNAs with covalently closed-loop structure, which provides its stability characteristics [11, 20]. Studies from the past several decades have revealed the function of part of circRNAs

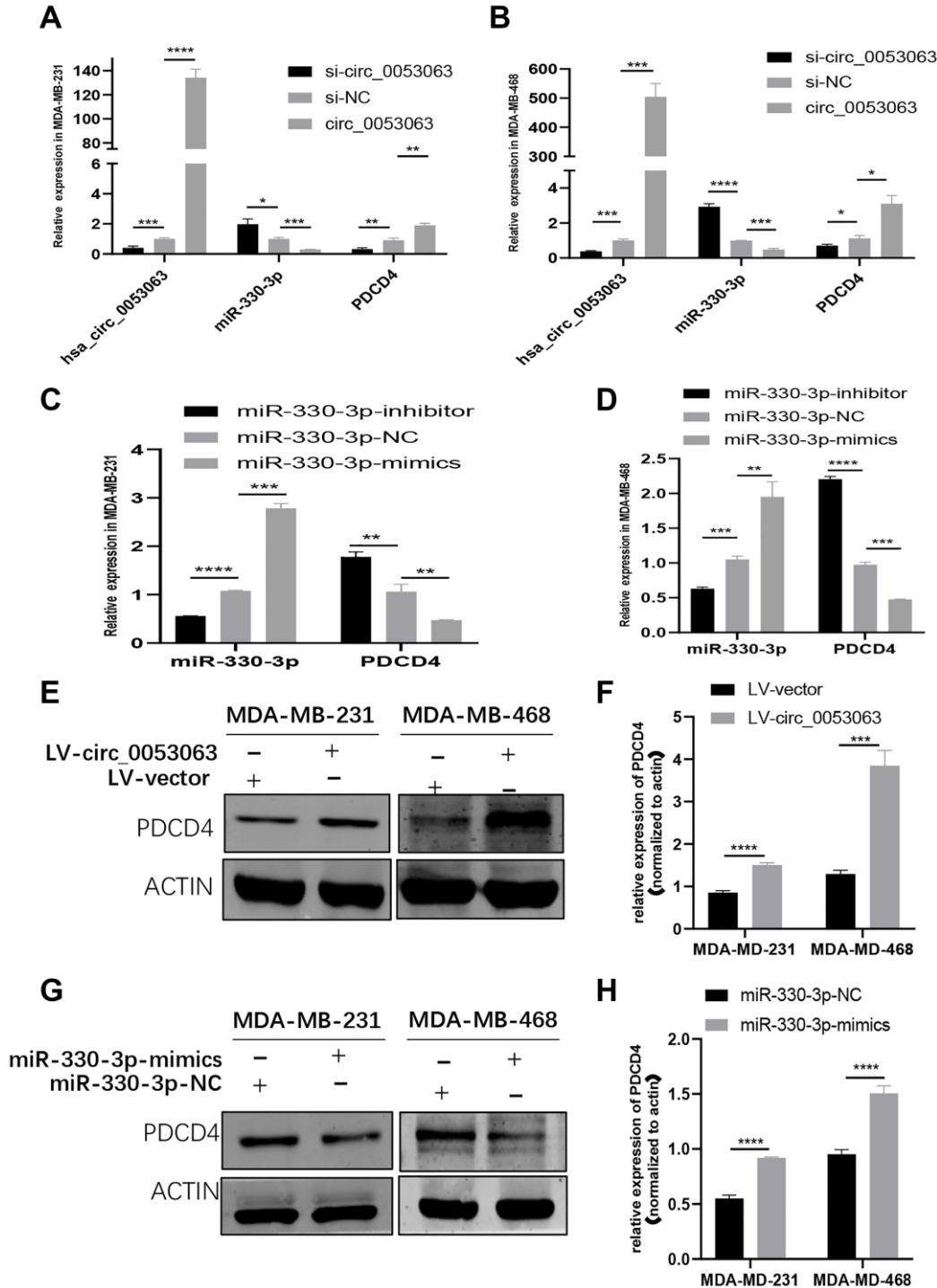


**Figure 7. Hsa\_circ\_0053063 activated PDCD4 through targeting miR-330-3p.** (A–B) qRT-PCR analysis revealed the expression of PDCD4 after transfecting miR-330-3p mimics, hsa\_circ\_0053063 siRNA, and LV-circ-0053063 in MDA-MB-231 and MDA-MB-468 cells. (C–D) qRT-PCR analysis revealed the expression of PDCD4 mRNA in MDA-MB-231 and MDA-MB-468 cells treated with miR-330-3p mimics and inhibitors. (E–F) Western blot assays were employed to detect the protein levels of PDCD4 in MDA-MB-231 and MDA-MB-468 cell lines transfected with lv-circ\_0053063. (G–H) Western blot assays were employed to detect the protein levels of PDCD4 in MDA-MB-231 and MDA-MB-468 cell lines transfected with miR-330-3p mimics. (\* $p < 0.05$ , \*\* $p < 0.01$ , \*\*\* $p < 0.001$ , \*\*\*\* $p < 0.0001$ ).

so that plentiful circRNAs have been uncovered to be vital in biological progress and may participate in the development of cancers [21, 22]. CircRNAs have no 5' caps and 3' poly-A tails causing their stability and long half-life [23]. Based on the above advantages, circRNAs may serve as better diagnostic biomarkers than other ncRNAs.

More and more evidence has been put forward on how circRNAs work as a miRNA sponge to execute its function to influence tumor progression [24]. For example, the miR-29b family was decoyed by

circRNA\_100290 to regulate CDK6 expression [25]. Also, circRNAs as a regulatory factor and a valuable diagnostic marker of BC have been proved. For instance, circ\_0001667 promoted BC cell proliferation and survival via regulating TAZ to influence the hippo pathway [26], hsa\_circ\_0001982 promoted BC cell carcinogenesis through diminishing miR-143 [27].

In this study, data from high throughput sequencing chip GSE101123 in the GEO database indicated that a circRNA, hsa\_circ\_0053063 may have a higher

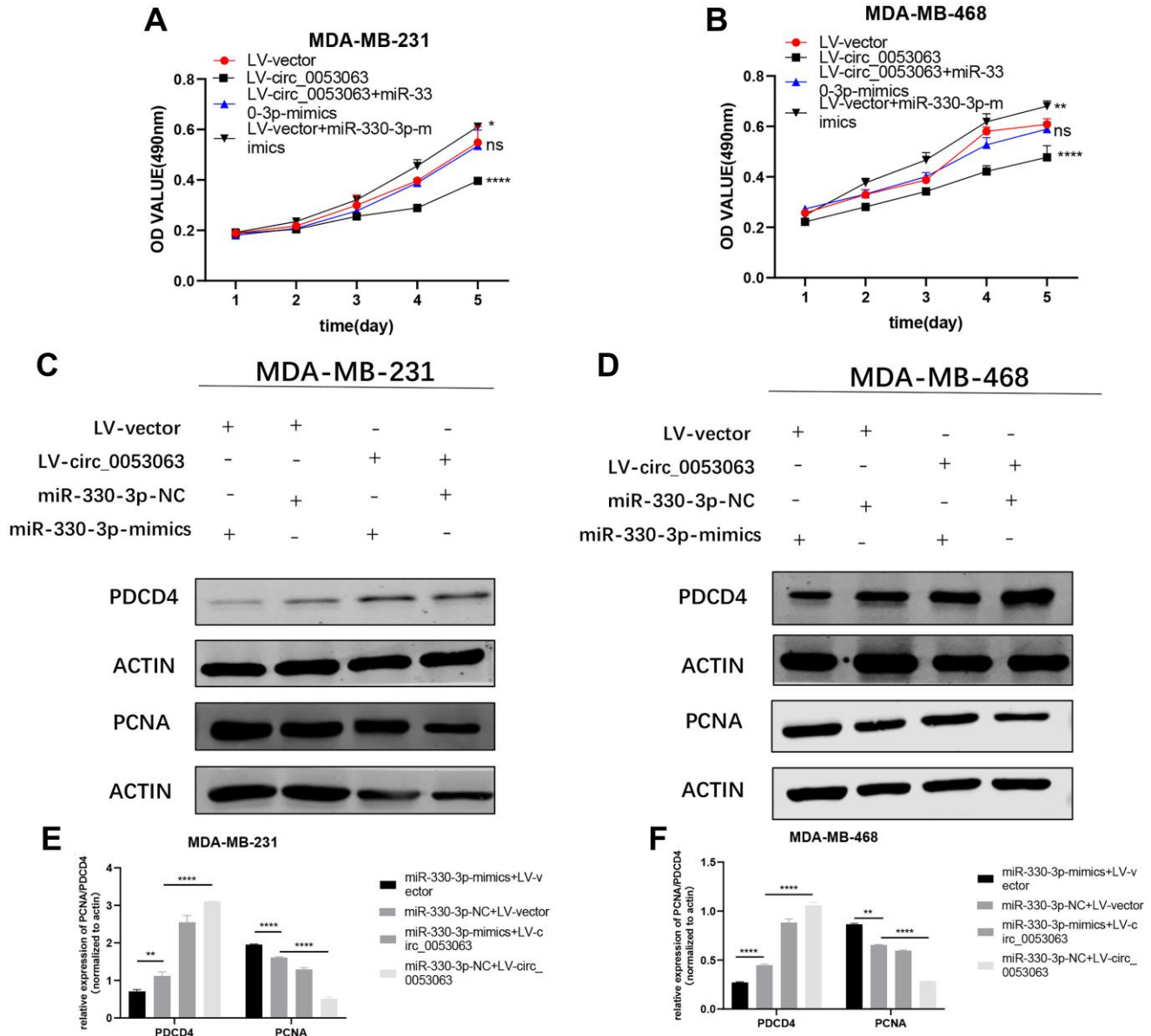


**Figure 8. Hsa\_circ\_0053063 generated the anti-oncogenic function in BC cells via the regulation of miR-330-3p/PDCD4 axis.** (A–B) Effect of LV-circ\_0053063 and miR-330-3p mimics on proliferation in MDA-MB-231 and MDA-MB-468 cell lines by MTT assay. (C–F) Western blot assay revealed the protein level of PDCD4 transfected with hsa\_circ\_0053063 and miR-330-3p mimics in MDA-MB-231 and MDA-MB-468 cell lines (\* $p < 0.05$ , \*\* $p < 0.01$ , \*\*\* $p < 0.001$ , \*\*\*\* $p < 0.0001$ ).

expression in BC tissues. Then qRT-PCR was performed to confirm that hsa\_circ\_0053063 was highly expressed in BC tissues as well as in BC cell lines. Moreover, the expression has a connection with the age of BC patients, suggesting that hsa\_circ\_0053063 may conduct as a diagnostic biomarker for aged BC patients. Through functional experiments, we found that over-expressed hsa\_circ\_0053063 significantly decreased cell viability and proliferation, by the contrary, si-

circ\_0053063 increased cell viability and proliferation. Moreover, we confirmed this *in vivo* through mice experiments. All results above demonstrated that hsa\_circ\_0053063 served as a cancer-suppressor in BC progression. MiR-330-3p has been predicted and validated as a target of hsa\_circ\_0053063. Studies have revealed the tumor accelerator function of miR-330-3p in BC [28]. To explore the underlying mechanism between hsa\_circ\_0053063 and miR-330-3p, we

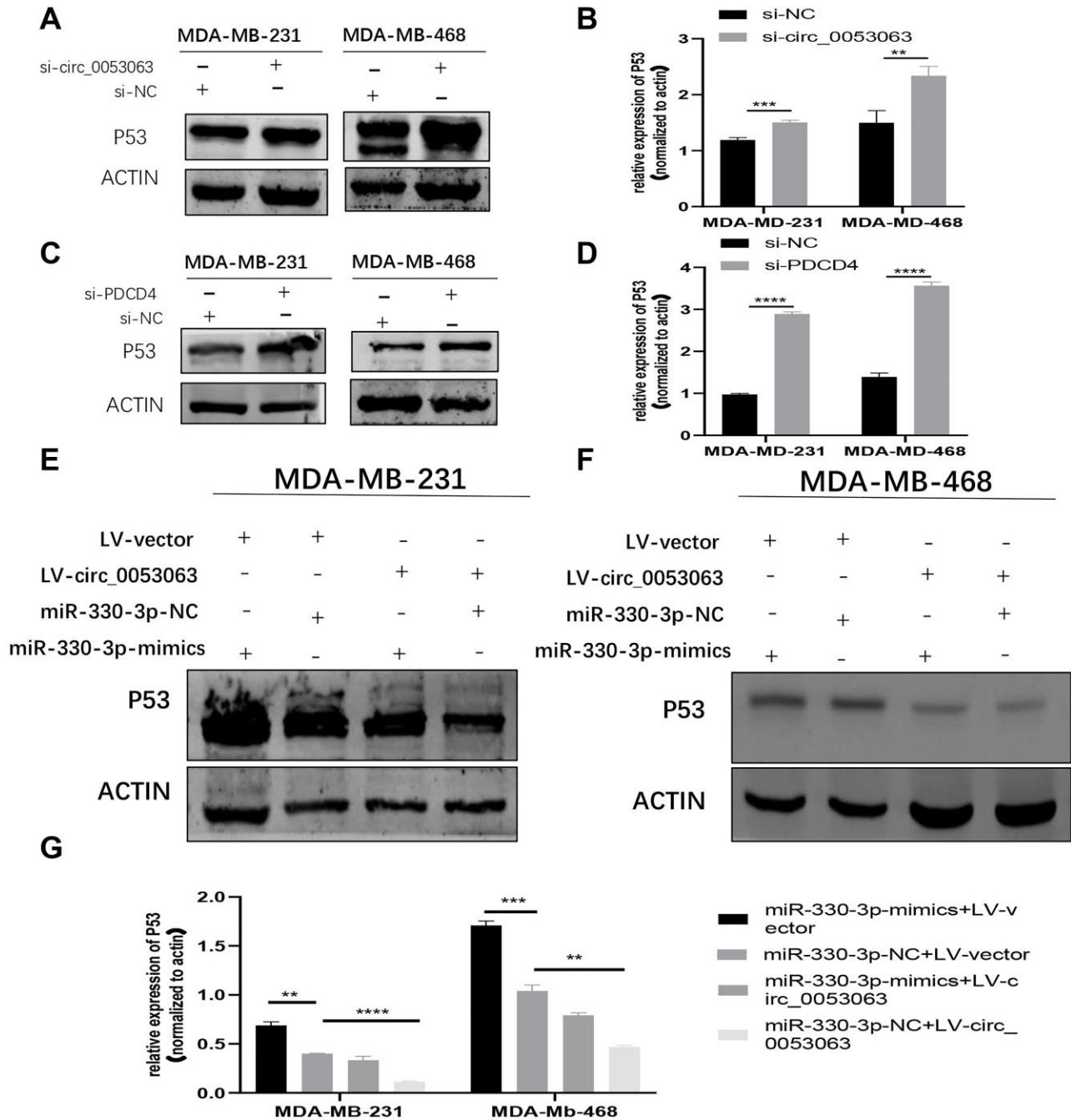


**Figure 9. Hsa\_circ\_0053063 inactivated P53 through miR-330-3p/PDCD4 axis.** (A–B) Western blot assay revealed the P53 protein level in MDA-MB-231 and MDA-MB-468 cells treated with hsa\_circ\_0053063 siRNA. (C–D) Western blot assay revealed the P53 protein level in MDA-MB-231 and MDA-MB-468 cell lines transfected with PDCD4 siRNA. (E–G) Western blot assay revealed the protein level of P53 in MDA-MB-231 and MDA-MB-468 cell lines transfected with hsa\_circ\_0053063 and miR-330-3p mimics. (\* $p < 0.05$ , \*\* $p < 0.01$ , \*\*\* $p < 0.001$ , \*\*\*\* $p < 0.0001$ ).

performed functional experiments and the results proved the correlations between them. Firstly, hsa\_circ\_0053063 was negatively correlated with miR-330-3p. Secondly, miR-330-3p mimics significantly increased cell viability and proliferation, indicating the ability of miR-330-3p to promote BC cell progression. Lastly, rescue experiments implied that hsa\_circ\_0053063-induced decreasing cell proliferation could be recovered by miR-330-3p mimics, demonstrating that hsa\_circ\_0053063 realized its anti-oncogene function by targeting miR-330-3p. However, the deep regulation mechanism under this hsa\_circ\_0053063/miR-330-3p axis is still unknown and needs to be further studied. Based on the researches before, PDCD4 is a tumor suppressor [29, 30]. In BC, PDCD4 has been proved to inhibit the BC cell invasion [31, 32]. Importantly, PDCD4 is predicted to be a putative gene of miR-330-3p by using databases. Therefore, hsa\_circ\_0053063 influences the regulation of PDCD4 through sponging miR-330-3p, thus regulating cell biological functions of BC. qRT-PCR was employed

to test the expression of PDCD4 in MDA-MB-231 and MDA-MB-468 cells transfected with si-circ\_0053063 and LV-circ\_0053063. Results indicated that LV-circ\_0053063 could significantly enhance the expression level of PDCD4, while si-circ\_0053063 was, on the contrary, demonstrated that hsa\_circ\_0052063 played a vital role in PDCD4 regulation. The function experiment showed the inhibitory effect of PDCD4 on the proliferation of BC. From the western blot assay, we proved that miR-330-3p promoted cell proliferation by inhibiting PDCD4. In general, the present study demonstrated that hsa\_circ\_0053063 was treated as a miR-330-3p sponge, and executed its function by removing the inhibitory effect of miR-330-3p on its target PDCD4, finally, regulating the expression of PDCD4.

P53 has been considered as an identified translational target of PDCD4 [19]. Further studies have proved that hsa\_circ\_0053063 could inhibit the P53 protein level through the miR-330-3p/PDCD4 axis.

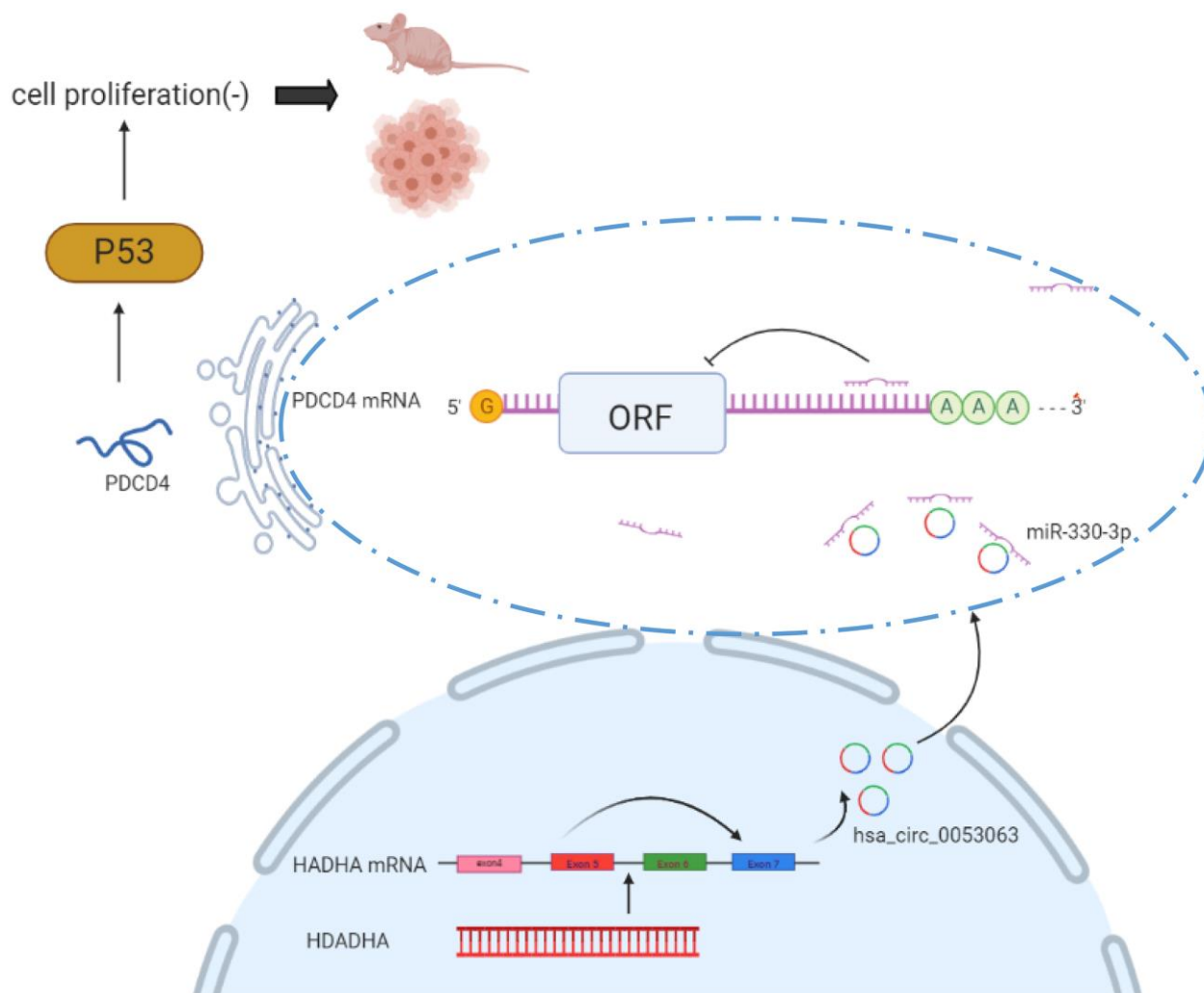


Figure 10. Mechanism diagram shows how hsa\_circ\_0053063 inhibits BC cell proliferation by miR-330-3p as a ceRNA.

Therefore, the discovery of hsa\_circ\_0053063 provides a PDCD4 accelerator, which may be a new diagnostic target and beneficial for BC patients in the further.

## CONCLUSIONS

In conclusion, we found a novel circRNA that is highly expressed in BC, hsa\_circ\_0053063. We revealed its underlying mechanism as a tumor suppressor to activate PDCD4 via serving as a sponge of miR-330-3p. These experiential results imply a new potential biomarker or therapeutic target for BC.

## MATERIALS AND METHODS

### Human BC tissue samples

30 pairs of tumor tissues and matched normal tissues from BC patients undergoing surgery were obtained from the Department of Breast and Thyroid Surgery of Shanghai Tenth People's Hospital (Shanghai, China). The clinical samples were immediately stored in liquid nitrogen after surgery. All patients had received no anti-tumor therapy before and the details of their clinical information were available. Both tumor tissue and adjacent non-tumor tissue were confirmed by specialized pathologists. Consents were given and this study was approved by the Institution Ethics Committees of Shanghai Tenth People's Hospital.

### Cell culture and actinomycin D treatment

MCF-10A cells, the human normal breast cells, were purchased from Zhongqiaoxin Zhou Biotech (Shanghai, China) and cultured in Mammary Epithelial Cell Medium (MEpiCM, ScienCell, Research Laboratories, Carlsbad, CA, USA). BC cell lines including MDA-MB-231, MCF-7, HCC-1937, SKBR3, MDA-MB-468 were purchased from the Chinese Academy of Sciences (Shanghai) and cultured in Dulbecco's Modified Eagle's Medium (DMEM) (Gibco, USA) adding 10% Fetal Bovine Serum (FBS) (Gibco), penicillin (100 U/ml) and streptomycin (100 µg/ml) (Enpromise, China). The cell cultural condition of the cell incubator was set at 37°C with 5% CO<sub>2</sub>. 2 µg/ml actinomycin D (Millipore, Billerica, MA, USA) was added to the DMEM to inhibit transcription of MDA-MB-231 and MDA-MB-468 cells for 0 h, 8 h, 16 h, and 24 h.

### Cell transfection and lentivirus transduction

Si-RNA specifically targeting hsa\_circ\_0053063 (si-circ\_0053063), and si-RNA negative control (si-NC) were purchased from IBSBio (Shanghai, China). MiR-330-3p-mimics, inhibitor, and miRNA negative control (miR-NC) were purchased from RiboBio (Guangzhou, China). PDCD4 siRNA was synthesized by Integrated Biotech

Solutions (Shanghai, China). Liposomal transfection reagent (Yeasen, Shanghai, China) was used for cell transfection. MDA-MB-231 and MDA-MB-468 cells were transfected with reagents mentioned above, according to the manufacturer's instructions. Plasmid extraction was finished by DNA Midiprep Kits (Qiagen, Hilden, Germany). A lentivirus plasmid containing circ\_0053063 was assembled by ZORIN (Shanghai, China).

### RNA extraction, reverse transcription and qRT-PCR

Nuclear and cytoplasmic RNA was extracted individually by the PARIS™ Kit (Invitrogen, Carlsbad, CA, USA). Total RNA of cells and tissues was extracted with TRIzol reagent (Invitrogen, Carlsbad, CA, USA). The RNA concentration and purity were assessed with a Nanodrop 2000 spectrophotometer (Thermo Fisher Scientific, Inc.). Reverse transcription was applied to obtain cDNA using HiScript III RT SuperMix kit (Vazyme Biotech, Nanjing, China). qRT-PCR was conducted on a 7900HT Fast RT-PCR instrument (Applied Biosystems, Singapore). Hieff® qPCR SYBR® Green Master Mix, the reagent for qRT-PCR, was purchased from Yeasen (Shanghai, China). Primers were produced by Sangon Biotech (Shanghai, China). 18S rRNA, U6 snRNA, and β-Actin (ACTB) were regarded as internal calibrators for hsa\_circ\_0053063, miRNA, and mRNA respectively. Primers used in this article are presented in Supplementary Table 1. The results of qRT-PCR were analyzed for relative quantitation using the 2-ΔΔCT method.

### RNase R resistance analysis of circRNAs

Total RNA from MDA-MB-231 and MDA-MB-468 cell lines were treated with RNase R (4 U/mg, Epicenter) according to the manufacturer's instruction and detected by the qRT-PCR assay.

### MTT assay

About 2000 transfected MDA-MB-231 and MDA-MB-468 cells were planted into 96-well-plates per well. The MTT assay kit (Sangon, Shanghai, China) was used to determine cell viability at 24 h, 48 h, 72 h, and 96 h. The crystal was dissolved in 150 µl dimethylsulfoxide (DMSO, Sangon, Shanghai, China) after 4-hours-incubation together with MTT reagent and the optical density (OD) value was measured at 490 nm using a microplate spectrophotometer (BioTek, Vermont USA).

### Colony formation assay

Transfected MDA-MB-231 and MDA-MB-468 cells were incubated for 10–14 days after seeding into 6-well-

plates (500 cells per well). When the cell colonies were visible, the plates were washed twice with phosphate-buffered saline (PBS, Sangon, Shanghai, China). The washed cell colonies were then fixed in 95% ethanol and stained with 0.1% crystal violet. Colony number was counted immediately after taking photographs.

### Dual-luciferase reporter assay

PmirGLO-hsa\_circ\_0053063 and pmirGLO-PDCD4 mutant and wild-type reporter plasmids were purchased from Integrated Biotech Solutions (Shanghai, China). 293T cells were planted in 24-well plates. When the confluency of the cells reached 80%, these plasmids were transfected as the transfection procedures used as above. After 24 hours, Dual-Luciferase Reporter Assay (Promega, Madison, WI, USA) was used to detect firefly and Renilla luciferase activities. Finally, the ratio of firefly/Renilla was calculated.

### Protein extraction and western blotting assay

Total proteins of cells were extracted by RIPA buffer (Beyotime, Shanghai, China) on the ice. The supernatants were obtained after centrifuging at 4°C, 12000 rpm for 30 min. The bicinchoninic acid (BCA) protein assay kit (Beyotime, Shanghai, China) was used to determine the concentration of proteins. The 6 × sodium dodecyl sulfate (SDS) loading buffer was added into proteins and the mixtures were boiled at 100°C for 10 min for protein denaturation. Equal masses of proteins from each sample were separated by electrophoresis on a 10% polyacrylamide SDS gel (Beyotime, Shanghai, China). The proteins were transferred onto 0.45 μm nitrocellulose membranes (Beyotime, Shanghai, China) and then blocked by 5% non-fatty milk for an hour. Primary antibodies were added to the membranes and incubated overnight. After washing 3 times (10 min per time) in PBST, (PBS with 0.1% Tween20), the blots were incubated with the secondary antibody (anti-mouse or anti-rabbit) for 60 min at room temperature. After washing with PBST, the membranes were detected by an Odyssey Scanning system (Li-Cor, USA) and measured by ImageStudio.

### FISH assay

The fluorescence *in situ* hybridization (FISH) probe of hsa\_circ\_0053063 was purchased from RiboBio (Guangzhou, China). The process of FISH followed the manufacturer's instructions. 4', 6-Diamidino-2-Phenylindole (DAPI) was used for nuclear staining. The photographs were captured by the Thermo Fisher microscope (Thermo Fisher Scientific, Massachusetts, USA).

### Immunohistochemical assay

The immunohistochemical assay was performed on formalin-fixed, paraffin-embedded (FFPE) nude mouse tissues. FFPE slides were cut and prepared. Antibody PDCD4 was used to do IHC following the protocol. The slides of two groups were observed under the microscope, and five different views were photographed randomly per slide.

### Xenograft tumor assay

4–6 weeks old athymic female nude mice which weighed between 18 to 22 g were ordered from the laboratory animal center of Shanghai. Almost  $1 \times 10^6$  MDA-MB-231 transfected with lv-circ\_0053063 or lv-NC were injected into the second mammary fat of each mouse (4 mice per group). Then, tumor size was measured and calculated every week. After 35 days, they were executed and their tumor lumps were collected immediately.

### Statistical analysis

The significant differences were assessed by GraphPad Prism V8.0 (GraphPad, CA, USA), SPSS 20.0 (IBM, SPSS, IL, USA), and RStudio (RStudio, MA, USA). Three independent experiment data were obtained and presented as the means ± standard deviation (SD). *P*-value < 0.05 was considered as significant results.

### Availability of data and materials

The datasets used and analyzed during the current study are available from the corresponding author on reasonable request.

### Ethics approval

Animal experiments were conducted in mice using protocols approved by the Ethics Committee of Shanghai Tenth People's Hospital of Tongji University, and written informed consent was obtained from all patients or their relatives.

### Abbreviations

circRNA: Circular RNA; ncRNA: Non-coding RNA; GEO: Gene Expression Omnibus; PDCD4: Programmed Cell Death 4; GAPDH: Glyceraldehyde-3-Phosphate Dehydrogenase; qRT-PCR: Quantitative real-time polymerase chain reaction; ceRNA: competing endogenous RNAs; HADHA: hydroxyacyl-CoA dehydrogenase trifunctional multienzyme complex subunit alpha.

## AUTHOR CONTRIBUTIONS

CJ and LF designed the research. CJ performed the research and analyzed the results. JH helped to perform the research. CJ wrote the paper. XW, XD, WZ, YY, KH, and XZ edited the manuscript and provided critical comments.

All authors read and approved the final manuscript.

## ACKNOWLEDGMENTS

The authors would like to acknowledge the helpful comments on this paper received from the reviewers.

## CONFLICTS OF INTEREST

The authors declare that they have no competing interests.

## FUNDING

This work was supported by the National Natural Sciences Foundation of China (grant no. 82073204), the Shanghai Municipal Health Bureau of Shanghai, China (Grant Number: 201640097), and the Shanghai Science and Technology Commission Guidance Project (Grant Number: 17411967200).

## REFERENCES

1. Bray F, Ferlay J, Soerjomataram I, Siegel RL, Torre LA, Jemal A. Global cancer statistics 2018: GLOBOCAN estimates of incidence and mortality worldwide for 36 cancers in 185 countries. *CA Cancer J Clin.* 2018; 68:394–424.  
<https://doi.org/10.3322/caac.21492>  
PMID:[30207593](https://pubmed.ncbi.nlm.nih.gov/30207593/)
2. Ginsburg O, Bray F, Coleman MP, Vanderpuye V, Eniu A, Kotha SR, Sarker M, Huong TT, Allemani C, Dvaladze A, Gralow J, Yeates K, Taylor C, et al. The global burden of women's cancers: a grand challenge in global health. *Lancet.* 2017; 389:847–860.  
[https://doi.org/10.1016/s0140-6736\(16\)31392-7](https://doi.org/10.1016/s0140-6736(16)31392-7)  
PMID:[27814965](https://pubmed.ncbi.nlm.nih.gov/27814965/)
3. Januskeviciene I, Petrikaite V. Heterogeneity of breast cancer: The importance of interaction between different tumor cell populations. *Life Sci.* 2019; 239:117009.  
<https://doi.org/10.1016/j.lfs.2019.117009>  
PMID:[31669239](https://pubmed.ncbi.nlm.nih.gov/31669239/)
4. Lee KL, Kuo YC, Ho YS, Huang YH. Triple-Negative Breast Cancer: Current Understanding and Future Therapeutic Breakthrough Targeting Cancer Stemness. *Cancers (Basel).* 2019; 11:1334.  
<https://doi.org/10.3390/cancers11091334>  
PMID:[31505803](https://pubmed.ncbi.nlm.nih.gov/31505803/)
5. Thakur V, Kutty RV. Recent advances in nanotheranostics for triple negative breast cancer treatment. *J Exp Clin Cancer Res.* 2019; 38:430.  
<https://doi.org/10.1186/s13046-019-1443-1>  
PMID:[31661003](https://pubmed.ncbi.nlm.nih.gov/31661003/)
6. Zheng Q, Cui X, Zhang D, Yang Y, Yan X, Liu M, Niang B, Aziz F, Liu S, Yan Q, Liu J. miR-200b inhibits proliferation and metastasis of breast cancer by targeting fucosyltransferase IV and alpha1,3-fucosylated glycans. *Oncogenesis.* 2017; 6:e358.  
<https://doi.org/10.1038/oncsis.2017.58>  
PMID:[28692034](https://pubmed.ncbi.nlm.nih.gov/28692034/)
7. Lin A, Li C, Xing Z, Hu Q, Liang K, Han L, Wang C, Hawke DH, Wang S, Zhang Y, Wei Y, Ma G, Park PK, et al. The LINK-A lncRNA activates normoxic HIF1alpha signalling in triple-negative breast cancer. *Nat Cell Biol.* 2016; 18:213–24.  
<https://doi.org/10.1038/ncb3295>  
PMID:[26751287](https://pubmed.ncbi.nlm.nih.gov/26751287/)
8. Yang J, Meng X, Yu Y, Pan L, Zheng Q, Lin W. LncRNA POU3F3 promotes proliferation and inhibits apoptosis of cancer cells in triple-negative breast cancer by inactivating caspase 9. *Biosci Biotechnol Biochem.* 2019; 83:1117–1123.  
<https://doi.org/10.1080/09168451.2019.1588097>  
PMID:[30843771](https://pubmed.ncbi.nlm.nih.gov/30843771/)
9. Yin Y, Long J, He Q, Li Y, Liao Y, He P, Zhu W. Emerging roles of circRNA in formation and progression of cancer. *J Cancer.* 2019; 10:5015–5021.  
<https://doi.org/10.7150/jca.30828>  
PMID:[31602252](https://pubmed.ncbi.nlm.nih.gov/31602252/)
10. Wang X, Fang L. Advances in circular RNAs and their roles in breast Cancer. *J Exp Clin Cancer Res.* 2018; 37:206.  
<https://doi.org/10.1186/s13046-018-0870-8>  
PMID:[30157902](https://pubmed.ncbi.nlm.nih.gov/30157902/)
11. Sanger HL, Klotz G, Riesner D, Gross HJ, Kleinschmidt AK. Viroids are single-stranded covalently closed circular RNA molecules existing as highly base-paired rod-like structures. *Proc Natl Acad Sci U S A.* 1976; 73:3852–6.  
<https://doi.org/10.1073/pnas.73.11.3852>  
PMID:[1069269](https://pubmed.ncbi.nlm.nih.gov/1069269/)
12. Kristensen LS, Andersen MS, Stagsted LVW, Ebbesen KK, Hansen TB, Kjems J. The biogenesis, biology and characterization of circular RNAs. *Nat Rev Genet.* 2019; 20:675–691.  
<https://doi.org/10.1038/s41576-019-0158-7>  
PMID:[31395983](https://pubmed.ncbi.nlm.nih.gov/31395983/)

13. Matsuhashi S, Watanabe T, Hori K. An antigen expressed in proliferating cells at late G1-S phase. *Exp Cell Res.* 1987; 170:351–62.  
[https://doi.org/10.1016/0014-4827\(87\)90312-0](https://doi.org/10.1016/0014-4827(87)90312-0)  
PMID:[3297740](https://pubmed.ncbi.nlm.nih.gov/3297740/)
14. Cmarik JL, Min H, Hegamyer G, Zhan S, Kulesz-Martin M, Yoshinaga H, Matsuhashi S, Colburn NH. Differentially expressed protein Pcd4 inhibits tumor promoter-induced neoplastic transformation. *Proc Natl Acad Sci U S A.* 1999; 96:14037–42.  
<https://doi.org/10.1073/pnas.96.24.14037>  
PMID:[10570194](https://pubmed.ncbi.nlm.nih.gov/10570194/)
15. Gao G, Liang X, Ma W. Sinomenine restrains breast cancer cells proliferation, migration and invasion via modulation of miR-29/PDCD-4 axis. *Artif Cells Nanomed Biotechnol.* 2019; 47:3839–3846.  
<https://doi.org/10.1080/21691401.2019.1666861>  
PMID:[31556312](https://pubmed.ncbi.nlm.nih.gov/31556312/)
16. Li C, Du L, Ren Y, Liu X, Jiao Q, Cui D, Wen M, Wang C, Wei G, Wang Y, Ji A, Wang Q. SKP2 promotes breast cancer tumorigenesis and radiation tolerance through PDCD4 ubiquitination. *J Exp Clin Cancer Res.* 2019; 38:76.  
<https://doi.org/10.1186/s13046-019-1069-3>  
PMID:[30760284](https://pubmed.ncbi.nlm.nih.gov/30760284/)
17. Li Y, Jiang D, Zhang Q, Liu X, Cai Z. Ubiquitin-specific protease 4 inhibits breast cancer cell growth through the upregulation of PDCD4. *Int J Mol Med.* 2016; 38:803–11.  
<https://doi.org/10.3892/ijmm.2016.2685>  
PMID:[27430936](https://pubmed.ncbi.nlm.nih.gov/27430936/)
18. Hui M, Kai W, Chen X, Guan X, Hu L, Xiong G, Li J, Yun B. MicroRNA-330-3p functions as an oncogene in human esophageal cancer by targeting programmed cell death 4. *Am J Cancer Res.* 2015; 5:1062–75.  
PMID:[26045986](https://pubmed.ncbi.nlm.nih.gov/26045986/)
19. Wedeken L, Singh P, Klempnauer KH. Tumor suppressor protein Pcd4 inhibits translation of p53 mRNA. *J Biol Chem.* 2011; 286:42855–62.  
<https://doi.org/10.1074/jbc.m111.269456>  
PMID:[22033922](https://pubmed.ncbi.nlm.nih.gov/22033922/)
20. Hsu MT, Coca-Prados M. Electron microscopic evidence for the circular form of RNA in the cytoplasm of eukaryotic cells. *Nature.* 1979; 280:339–40.  
<https://doi.org/10.1038/280339a0>  
PMID:[460409](https://pubmed.ncbi.nlm.nih.gov/460409/)
21. Du WW, Yang W, Liu E, Yang Z, Dhaliwal P, Yang BB. Foxo3 circular RNA retards cell cycle progression via forming ternary complexes with p21 and CDK2. *Nucleic Acids Res.* 2016; 44:2846–58.  
<https://doi.org/10.1093/nar/gkw027>  
PMID:[26861625](https://pubmed.ncbi.nlm.nih.gov/26861625/)
22. Guarnerio J, Bezzi M, Jeong JC, Paffenholz SV, Berry K, Naldini MM, Lo-Coco F, Tay Y, Beck AH, Pandolfi PP. Oncogenic Role of Fusion-circRNAs Derived from Cancer-Associated Chromosomal Translocations. *Cell.* 2016; 165:289–302.  
<https://doi.org/10.1016/j.cell.2016.03.020>  
PMID:[27040497](https://pubmed.ncbi.nlm.nih.gov/27040497/)
23. Chen LL, Yang L. Regulation of circRNA biogenesis. *RNA Biol.* 2015; 12:381–8.  
<https://doi.org/10.1080/15476286.2015.1020271>  
PMID:[25746834](https://pubmed.ncbi.nlm.nih.gov/25746834/)
24. Kulcheski FR, Christoff AP, Margis R. Circular RNAs are miRNA sponges and can be used as a new class of biomarker. *J Biotechnol.* 2016; 238:42–51.  
<https://doi.org/10.1016/j.jbiotec.2016.09.011>  
PMID:[27671698](https://pubmed.ncbi.nlm.nih.gov/27671698/)
25. Chen L, Zhang S, Wu J, Cui J, Zhong L, Zeng L, Ge S. circRNA\_100290 plays a role in oral cancer by functioning as a sponge of the miR-29 family. *Oncogene.* 2017; 36:4551–4561.  
<https://doi.org/10.1038/onc.2017.89>  
PMID:[28368401](https://pubmed.ncbi.nlm.nih.gov/28368401/)
26. Geng Z, Wang W, Chen H, Mao J, Li Z, Zhou J. Circ\_0001667 promotes breast cancer cell proliferation and survival via Hippo signal pathway by regulating TAZ. *Cell Biosci.* 2019; 9:104.  
<https://doi.org/10.1186/s13578-019-0359-y>  
PMID:[31893023](https://pubmed.ncbi.nlm.nih.gov/31893023/)
27. Tang YY, Zhao P, Zou TN, Duan JJ, Zhi R, Yang SY, Yang DC, Wang XL. Circular RNA hsa\_circ\_0001982 Promotes Breast Cancer Cell Carcinogenesis Through Decreasing miR-143. *DNA Cell Biol.* 2017; 36:901–908.  
<https://doi.org/10.1089/dna.2017.3862>  
PMID:[28933584](https://pubmed.ncbi.nlm.nih.gov/28933584/)
28. Mesci A, Huang X, Taeb S, Jahangiri S, Kim Y, Fokas E, Bruce J, Leong HS, Liu SK. Targeting of CCBE1 by miR-330-3p in human breast cancer promotes metastasis. *Br J Cancer.* 2017; 116:1350–1357.  
<https://doi.org/10.1038/bjc.2017.105>  
PMID:[28419078](https://pubmed.ncbi.nlm.nih.gov/28419078/)
29. Lankat-Buttgereit B, Göke R. The tumour suppressor Pcd4: recent advances in the elucidation of function and regulation. *Biol Cell.* 2009; 101:309–17.  
<https://doi.org/10.1042/bc20080191>  
PMID:[19356152](https://pubmed.ncbi.nlm.nih.gov/19356152/)
30. Yang HS, Jansen AP, Komar AA, Zheng X, Merrick WC, Costes S, Lockett SJ, Sonenberg N, Colburn NH. The transformation suppressor Pcd4 is a novel eukaryotic translation initiation factor 4A binding protein that inhibits translation. *Mol Cell Biol.* 2003; 23:26–37.



<https://doi.org/10.1128/mcb.23.1.26-37.2003>

PMID:[12482958](https://pubmed.ncbi.nlm.nih.gov/12482958/)

31. González-Villasana V, Nieves-Alicea R, McMurtry V, Gutiérrez-Puente Y, Tari AM. Programmed cell death 4 inhibits leptin-induced breast cancer cell invasion. *Oncol Rep.* 2012; 27:861–6.

<https://doi.org/10.3892/or.2011.1600>

PMID:[22200873](https://pubmed.ncbi.nlm.nih.gov/22200873/)

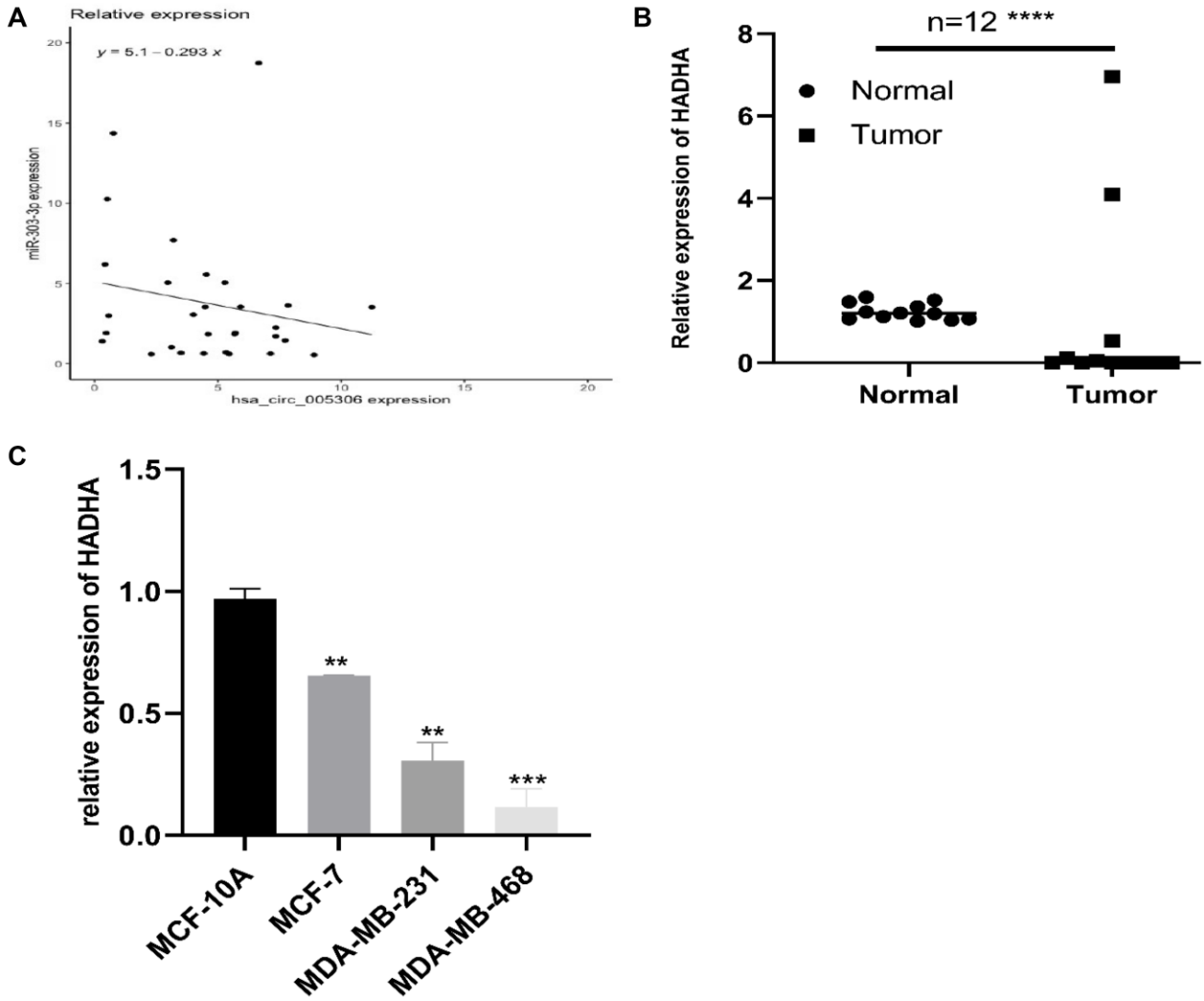
32. Nieves-Alicea R, Colburn NH, Simeone AM, Tari AM. Programmed cell death 4 inhibits breast cancer cell invasion by increasing tissue inhibitor of metalloproteinases-2 expression. *Breast Cancer Res Treat.* 2009; 114:203–9.

<https://doi.org/10.1007/s10549-008-9993-5>

PMID:[18386173](https://pubmed.ncbi.nlm.nih.gov/18386173/)

SUPPLEMENTARY MATERIALS

Supplementary Figure



Supplementary Figure 1. Relationship between hsa\_circ\_0053063 and miR-330-3p and relative expression of HADHA in breast cancer tissues and breast cancer cell lines.

## Supplementary Table

**Supplementary Table 1. Primers and siRNAs used in this study.**

PDCD4 siRNA	Sense	5'-GGAGCGUUUGUAGAAGAAdTdT-3'
	Antisense	3'-dTdTCCUCGCCAAACAUCUUCUU-5'
PDCD4	Forward	5'-TCGTCGTTACGATTGGTTAGTC-3'
	Reverse	5'-GAAAAATCTCTAACCCTTCTCGC-3'
Has_circ_0053063	Forward	5'-CAAGACCCTTCAAGAAGTAACAC-3'
	Reverse	5'-AACCTCAAGTCCTCCTCCC-3'
GAPDH	Forward	5'-CAGGAGGCATTGCTGATGAT-3'
	Reverse	5'-GAAGGCTGGGGCTCATTT-3'
U6	Forward	5'-CAAATTCGTGAAGCGTCCATAT-3'
	Reverse	5'-GCTTACGAATTTGCGTGTCATCCTTGC-3'
18S rRNA	Forward	5'-GGACATCTAAGGGCATCACAG-3'
	Reverse	5'-GAGACTCTGGCATGCTAACTAG-3'